Hydrodynamic Mapping of Two-Dimensional Electric Fields in Monolayers

Pierre Nassoy, William R. Birch, David Andelman,* and Francis Rondelez

Laboratoire de Physico-Chimie des Surfaces et Interfaces, Institut Curie, 11 Rue Pierre et Marie Curie, F-75231 Paris Cedex 05, France

(Received 10 July 1995)

We have measured the 2D dipolar electric fields generated by surface density fluctuations in Langmuir monolayers using optical microscopy to monitor the motion of micron-size, electrically charged, particles trapped at the air-water interface. The particle velocity is directly proportional to the local electric field gradient. Quantitative agreement with the theory is demonstrated for charged polystyrene latex particles interacting with liquid condensed domains of pentadecanoic acid. Typical velocities are of order 0.1–10 μm/s, corresponding to forces in the 10^{-15}–10^{-12} N range.

PACS numbers: 68.10.–m, 47.65.+a, 82.70.Kj, 87.22.Bt

Despite the key role played by electric fields in numerous interfacial physical and biological phenomena, such as electrostatic adhesion [1], voltage-gated ion transport in cell membranes, and nerve impulse propagation [2], very few attempts to probe the local electric potentials have been reported. Indeed, although theoretical calculations for model systems can be solved at least numerically, nondisruptive experimental observations are more difficult to achieve and often require sophisticated instrumentation. In this respect the recent report by Shikin of optical mapping of surface potentials in helium films, obtained by depositing electrons at the liquid/gas interface, is quite an achievement [3].

In this paper, we present a hydrodynamic method which provides both direct visualization and quantitative measurement of local electric fields in thin films of organic molecules. Here we have chosen to investigate Langmuir monolayers of fatty acids but the same methodology can be applied to phospholipid monolayers, biological membranes, etc., i.e., in all the cases where density fluctuations and/or insertion of charged proteins are likely to create nonuniform electric field distributions [4]. On the one hand, regions of higher surface density than their surrounding can be viewed as macrodipoles, the values of which are the vectorial sum of all the individual molecular dipoles. On the other hand, charged proteins create Coulombic electric fields around them. The central idea of our method is to incorporate in the monolayer a few micron-size particles, carrying a net dipole moment, and to record their motion by using optical microscopy. The measured velocity is directly proportional to the drag force and, therefore, to the local electric field gradient.

Let us consider a Langmuir monolayer in its two-phase liquid condensed (LC) and liquid expanded (LE) coexistence region. Because of the difference in surface densities the LC domains possess an excess dipole density $\overrightarrow{\mu_d}$ with respect to the surrounding LE phase. This is the very reason why periodic superstructures (supercrystals of hexagonal symmetry or stripe phases) can be formed in insoluble monolayers via long-range dipole-dipole interactions [5] and why LC domains can be displaced laterally on the interface by external electric field gradients [6]. As we will show later we have to consider only the vertical component $\overline{\mu_d}$. The electric field generated at distance r from the border of one domain is then

$$E(\rho) = 2\frac{\overline{\mu_d}}{4\pi\varepsilon\varepsilon_0}\frac{1}{R}\left[\frac{(1+\rho^2)^{1/2}}{\rho} - \frac{[1+(\rho+2)^2]^{1/2}}{\rho+2}\right], \quad (1)$$

where ε is the effective dielectric constant of the medium, R is the radius of the domain, and $\rho = r/R$ [7].

Let us then calculate the dipole associated with a latex particle of radius a trapped at the air/water interface and uniformly coated with sulfonic acid groups (surface density $\overline{Q_p}$). As shown by Pieranski [8], if the beads are partially immersed in the aqueous subphase, the ionizable groups will be dissociated only on the submerged section of the bead, resulting in an asymmetric charge distribution. Together with the counterions, this gives rise to an electric double layer and hence to an effective macroscopic dipole $\vec{\mu}_p$ *oriented normal to the water surface,* and of order $\pi a^2\overline{Q_p}e\lambda_D$. Here λ_D is the Debye screening length $\approx(3\ \text{Å})/\sqrt{c_{\text{salt}}}$, where c_{salt} is the salt concentration in mol/l.

The energy acquired by the dipolar probe is given by the scalar product between the field $\vec{E}(\rho)$ and the dipole $\vec{\mu}_p$, $W_d(\rho) = \vec{\mu}_p \cdot \vec{E}(\rho)$. Since $\vec{\mu}_p$ is perpendicular to the interface, the interaction energy W_d depends only on the vertical component of the electric field as expressed in Eq. (1).

The particle velocity $v(\rho)$ in the plane of the interface is obtained by balancing the dipolar force $F_d(\rho) = -R^{-1}dW_d(\rho)/d\rho$ with the viscous force $3\pi\eta a v$ [9]. The prefactor 3π comes from the boundary conditions of the Navier-Stokes equation for half-immersed beads [10], while η is the subphase viscosity ($\eta = 10^{-2}$ P for water).

This yields

$$v(\rho) = \frac{2}{3\pi\eta a}\,\frac{\mu_p\overline{\mu_d}}{4\pi\varepsilon\varepsilon_0}\,\frac{1}{R^2} \times \left[\frac{1}{\rho^2(1+\rho^2)^{1/2}} - \frac{1}{(\rho+2)^2[1+(\rho+2)^2]^{1/2}}\right]. \quad (2)$$

Since $v = Rd\rho/dt$, Eq. (2) is a differential equation whose integral will be used to determine $\rho(t)$. The energy $W_d(\rho)$ can be calculated by using the literature values for the various parameters. The dielectric constant of water is $\varepsilon \approx 7$ near the air/water boundary [11]. For carboxylic acids the perpendicular molecular dipole is equal to -0.15 D (pointing upwards) on an aqueous subphase of pH 2 [12]. Since the molecular cross section in the LC phase is 20 Å^2, this yields $\overline{\mu_d} = -7.5 \times 10^{-3}$ D/Å^2. For the polystyrene (PS) spheres commercially available, the surface charge density $\overline{Q_p}$ corresponds to one charge per 300 ± 100 Å^2. For a bead of radius 1.4 μm, the estimated particle dipole moment is therefore $\mu_p = 3 \times 10^9$ D (pointing towards the water) taking $\lambda_D \approx 30$ Å for the acidified ($10^{-2}M$ HCl) subphase. Figures 1(a) and 1(b) display the calculated dipole-dipole energy W_d and probe velocity v vs the distance r for three typical domain radii: 10, 25, and 50 μm. We note that the interaction is attractive over the whole range of separation distances, consistent with the fact that the dipoles of the bead and the LC domain have opposite orientations, and that W_d markedly exceeds k_BT up to distance $r \approx 3R$. The velocity can be described by simple power laws in the limit of very small and very large r, respectively. In the first case, the domain is equivalent to a semi-infinite wall and the velocity is proportional to $1/r^2$. In the second case, both the bead and the domain behave like point dipoles and the velocity decays as $1/r^4$. At intermediate distances, there is a smooth crossover between those two power laws. Line segments with slopes -2 and -4 are shown in Fig. 1(b) (log-log plot). We also observe that the calculated sphere velocities are in the range 0.1 to 20 μm/s, which is well within the capabilities of our optical detection.

The PS latex beads were purchased from Sigma in the form of aqueous solutions stabilized by surfactant and were extensively dialyzed against pure water just before use. Their contact angle with water was observed to be between 90° and 120°. Langmuir monolayers of pentadecanoic acid were spread on ultrapure water at pH 2 at an area per molecule of 40 Å^2, corresponding to the homogeneous LE phase [13] and to a surface pressure of 1 mN/m. A few droplets of the dilute bead suspension were then deposited at the interface and the monolayer was subsequently compressed until LC domains of size 10–50 μm were nucleated. The monolayer was visualized by epifluorescence microscopy using a metallurgical microscope equipped with a 40× objective and a video camera. The monolayer was doped with 1% of NBD-HDA (from Molecular Probes) as fluorescent markers. Preferential partitioning of the dye between the LE and LC regions makes the LC domains appear as dark disks in a background of bright LE phase. The spheres in the monolayer were detected as bright dots floating at the air-water interface and at random positions with respect to the LC domains. Their positions were recorded on a videotape and the sequences were later analyzed with an image analysis software. Careful elimination of convective flows [6(b)] leads to spatial and temporal resolutions of 1.5 μm and 0.05 s, respectively.

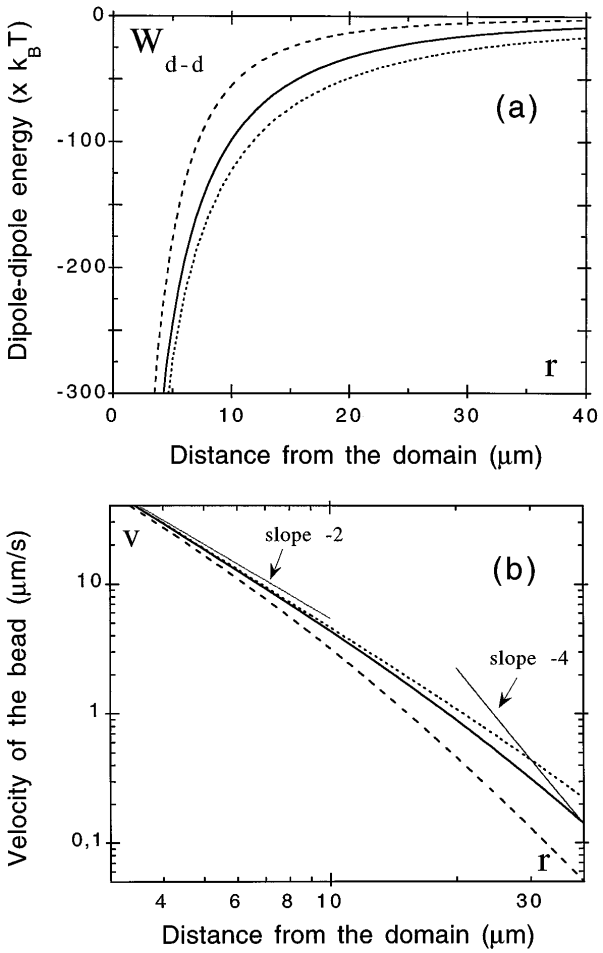

FIG. 1. (a) Calculated dipole-dipole interaction energy vs separation distance between a particle of radius $a = 1.4$ μm bearing a dipole $\mu_p = 3 \times 10^8$ D and a square LC domain of side length $2R$: (dashed line) $R = 10$ μm, (solid line) $R = 50$ μm with a dipolar density $\overline{\mu_d} = -0.75$ D/100 Å^2. (b) Log-log plot of the calculated bead velocity v as a function of the distance r.

Figure 2 shows three snapshots, taken at successive times, of a 1.4 μm radius bead interacting with an isolated LC domain of 22.5 μm in radius. Since the images were taken at decreasing intervals, one can see that the sphere is moving towards the LC domain at accelerated speeds as

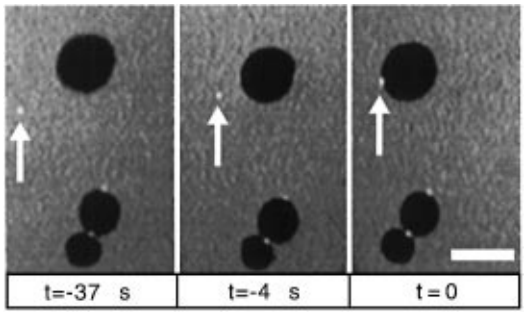

FIG. 2. Snapshots of a 1.4 μm polystyrene bead (white dot) approaching a LC domain of pentadecanoic acid (dark disk) in a Langmuir monolayer on an aqueous subphase of pH 2. Scale bar is 50 μm and domain radius is 22.5 μm. The origin of time $t = 0$ is the time at which contact is established. After contact the bead stays trapped at the LE-LC boundary. It can later serve as an attachment point for a second LC domain (see, for instance, the two domains at the bottom of the image).

it gets closer to the domain. It takes 33 s to move from 35 to 16 μm and 4 s only to move from 16 μm to contact. After contact, the bead remains trapped at the LE/LC interface. On the other hand, no attraction is detected, and the bead appears immobile if the bead-to-domain distance is larger than 100 μm. It is therefore always possible to select a bead which interacts with a single domain, which greatly simplifies the experiment. We have also verified by triangulation that the LC domains keep their relative positions during the bead displacement.

Figure 3 displays typical time evolutions of the position of a 1.4 μm bead interacting with a 25 μm radius LC domain. In each case the collection of data points comes from the video analysis of three independent events. Curves A and B correspond to pure and salted (0.2M NaCl) water subphase, respectively. Curve C corresponds to a particular case in which the bead is a 1.4 μm carboxylate-modified latex (CML) particle bearing no electrical surface charges. Several points are immediately apparent: (i) attraction between the charged bead and the LC domains is felt at large distances (20–30 μm); (ii) the velocity $v = dr/dt$ increases as the bead comes closer to the domain and reaches its maximum value (up to 10 μm/s); (iii) attraction is considerably less in the presence of the monovalent salt and is nonexistent for uncharged beads, even over the longest experimental times (several minutes) and for distances as small as 3 μm from the boundary. All these observations are consistent with an electrostatic interaction between the LC domain and the charged sphere. The solid lines are best fits to the data points obtained by numerically integrating Eq. (2) where the bead is considered as a point dipole [14] and the domain as an array of dipoles. The bead dipole moment μ_p is the only adjustable parameter, since the other parameters of Eq. (2), $\overline{\mu_d}$, ε, and η, are known from the literature. The μ_p values derived from the fit are found to be 3.1×10^8 and 0.7×10^8 D for curves A and B, respectively, and are in excellent agreement with

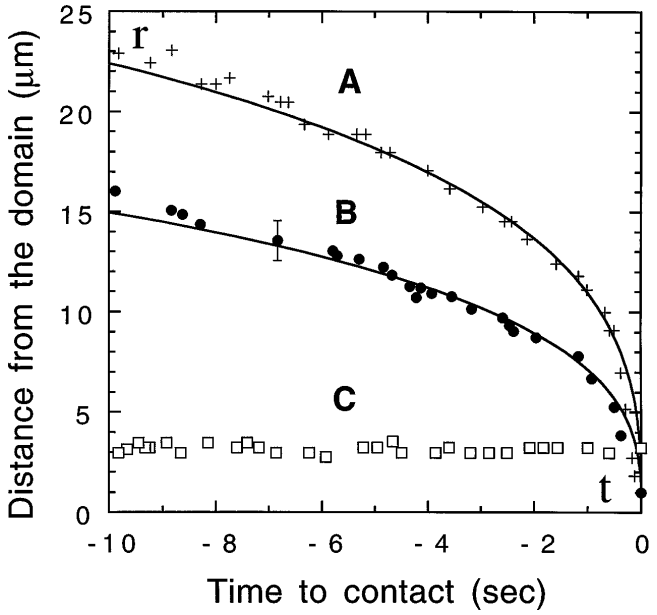

FIG. 3. Influence of the screening conditions on the displacement of a 1.4 μm bead interacting with a LC domain of radius 25 μm. Curves A and B correspond to a polystyrene bead on an acidified (pH 2) aqueous subphase, with no added salt and 0.2M NaCl salt, respectively. Curve C corresponds to a carboxylate-modified bead, bearing no surface charges. The solid lines are best fits by the function $r(t)$ obtained by integrating Eq. (2) and taking the bead dipole moment μ_p as the only adjustable parameter. A typical error bar in the bead position is shown on curve B.

the calculated value $\mu_p = \pi a^2 \overline{Q_p} e \lambda_D$, taking the Debye lengths λ_D equal to 30 and 7 Å in pure and salted water, respectively.

The excellent agreement between the experimental points of the bead velocities and the predictions of the dipolar model has encouraged us to try and calculate the interfacial electric field surrounding the LC domains. Indeed we know that the velocity of the bead is proportional to the local electric field gradient. Therefore a simple integration of the velocity-distance curve yields the local field at each point on the bead trajectory. There are several ways to achieve this integration; here we have selected a cubic spline operation followed by a numerical integration because it provides a direct knowledge of the electric field without any *a priori* assumption of its spatial dependence. Figure 4 gives the calculated values for the interfacial electric fields generated by a LC domain of 25 μm radius as a function of the distance to the edge of the domain (between 0 and 20 μm). Each data point was derived from the position versus time measurements of Figs. 3(a) and 3(b). Because of the circular symmetry of the system, a polar plot is sufficient to get the complete map. The absolute values of the electric field have been derived assuming half-immersed beads of radius $a = 1.4$ μm and the nominal surface charge density $\overline{Q_p} = (300\ \text{Å}^2)^{-1}$. We observe that the electric field varies from 0 to about 30 V/cm, with a rapid increase

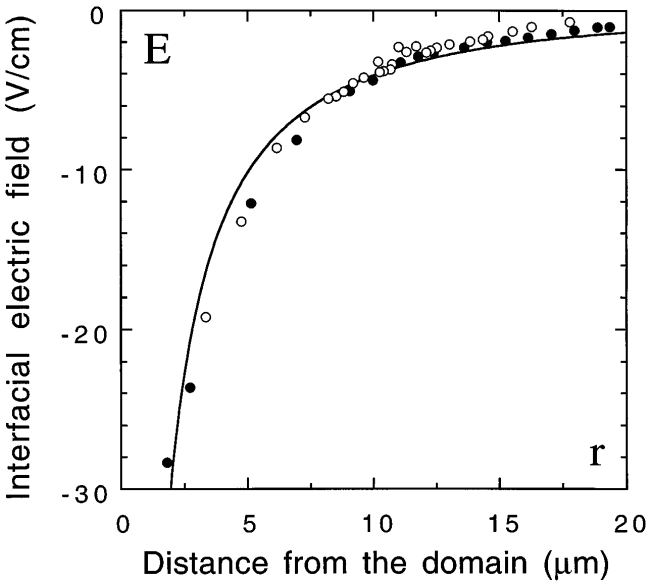

FIG. 4. Interfacial electric field created by a LC domain of radius $R = 25\ \mu$m vs distance. The open and full circles are the electric field values deduced from the bead velocity measurements on the salted and pure water [respectively, Figs. 3(a) and 3(b)], according to a numerical integration of Eq. (2): $t = \int_0^r dr/v(r)$. It is important to note that these values are model independent. The solid line is drawn according to Eq. (1).

at distances shorter than 5 μm. The solid line is the curve drawn using Eq. (1) for the distance dependence. It agrees extremely well with the values calculated from the velocity data, thus proving the validity of this hydrodynamic method to measure the electric fields. We observe that the E field generated by the LC domain on the pure and the salted subphase, respectively, are quite similar, even though the velocities at any given distance are markedly different. This result, which suggests that the electric field is not significantly screened by the counterions of the subphase, is by no means trivial and indicates that the molecular dipoles of the pentadecanoic acid are not in intimate contact with the water subphase. This will be discussed in more details in a forthcoming paper.

Our results give evidence that two-dimensional electric fields distributions in molecularly thin fluid systems can be deduced from velocity measurements of floating latex particles of micron size and bearing ionizable groups. In the particular case of Langmuir monolayers we have shown that the measurements are in quantitative agreement with the dipolar field generated by the excess surface charge densities contained within the LC domains. The values of the measured electric fields are in the range $1–10^2$ V/cm.

The method is exceptionally sensitive. Bead velocities of 0.1 μm/s, which are easily detectable by optical microscopy, correspond to forces of the order of 10^{-15} N. By comparison, force measurements using atomic force microscopy are currently limited to 10^{-11} N [15]. The bottom line of our hydrodynamic approach is that the work W dissipated in the process must be larger than k_BT. Therefore weak forces F have to be applied over sufficiently long distances l to ensure that $W = Fl > kT$; however, this puts no restriction on the absolute value of the forces that can be measured. The field distributions around proteins bearing typically 1000 electrical charges in biological membranes should be within experimental reach.

This work has been supported by Elf-Aquitaine (Direction de la Recherche, Technique et Environment) and by the Indo-French Center for Promotion of Advanced Research (IFCPAR) under Contract No. IFC907-2/94/2036. One of us (D. A.) would like to thank the Henri de Rothschild Foundation for a fellowship during his stay at the Curie Institute.

*Permanent address: School of Physics and Astronomy, Raymond and Beverly Sackler Faculty of Exact Sciences, Tel-Aviv University, Ramat-Aviv 69978, Israel.

[1] S. Duinhoven, R. Poort, G. Van der Voet, W. G. M. Agterof, W. Norde, and J. Lyklema, J. Colloid Interface Sci. **170**, 340 (1995).
[2] B. Alberts, D. Bray, J. Lewis, J. Raff, K. Roberts, and J. D. Watson, *Molecular Biology of the Cell* (Garland Publishing, New York, London, 1989).
[3] V. B. Shikin, Fiz. Nizk. Temp. **20**, 1158 (1994).
[4] P. Fromherz and J. U. Müller, Ber. Bunsen-Ges. Phys. Chem. **97**, 1071 (1993).
[5] (a) H. M. McConnell, Annu. Rev. Phys. Chem. **42**, 171 (1991); (b) D. Andelman, F. Brochard, and J. F. Joanny, J. Chem. Phys. **88**, 3873 (1987).
[6] (a) A. Miller and H. Möhwald, Europhys. Lett. **2**, 67 (1986); (b) J. F. Klingler and H. M. McConnell, J. Phys. Chem. **97**, 2962 (1993).
[7] Equation (1) is strictly valid for a square domain of side length $2R$. We have checked numerically by integrating its Taylor development up to sixth order that it remains an excellent approximation (to better than 10^{-3} for $r > 2\ \mu$m) for circular domains of radius R', provided the conversion factor $R' = (2/\sqrt{\pi})R$ is used.
[8] P. Pieranski, Phys. Rev. Lett. **45**, 569 (1980).
[9] The low Reynolds number of the system, Re $< 10^{-4}$, justifies this laminar flow approximation. Moreover, the small mass of the sphere ($\approx 10^{-14}$ kg) allows one to neglect inertia effects.
[10] L. Landau and E. Lifshitz, *Fluid Mechanics* (Pergamon Press, Oxford, 1984).
[11] R. J. Demschack and T. Fort, Jr., J. Colloid Interface Sci. **46**, 191 (1974).
[12] V. Vogel and D. Möbius, J. Colloid Interface Sci. **46**, 191 (1988).
[13] S. Akamatsu and F. Rondelez, J. Phys. II (France) **1**, 1309 (1991).
[14] The point approximation for the bead is valid to within 0.5% at all distances larger than 4.5 μm.
[15] V. T. Moy, E.-L. Florin, and H. E. Gaub, Science **266**, 257 (1994).